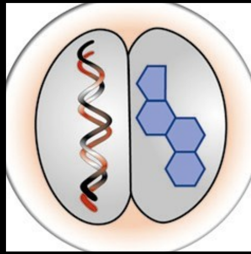

Endocrinology & Reproductive Physiology Program Annual Symposium

Monday, April 12, 2010

Fluno Center, University of Wisconsin—Madison

Table of Contents

Table of Contents *Page 2*

Program Agenda *Page 3*

Keynote Speaker Bio and Abstract *Page 4*

Faculty Speaker Bio and Abstract *Page 5*

Abstracts for Trainee Talks *Page 6*

Poster Session Abstracts *Page 11*

ERP Program Faculty Directory *Page 37*

2010 ERP Program Student Directory *Page 40*

NIH T32 Trainees *Page 40*

Acknowledgements

- The Endocrinology & Reproductive Physiology Program
- National Institutes of Health, NICHD Training Grant T32HD041921
- Abstract Book designed by Tiffany Bachmann, MA, Student Services Coordinator

2009/2010 Symposium Organizing Committee

- Dr. Manish Patankar, Chair
- Omar Jobe
- Carly Kibbe
- Brian Kenealy
- Soraya Silva
- Dr. Chanel Tyler, MD
- Dr. Ian Bird, Program Director (ex-officio member)

Program Schedule - Monday, April 12, 2010

9:00 am – 9:30 am	Registration and Poster set-up Location: Fluno Center Foyer
9:30 am	Welcome and Introduction of Invited Faculty Speaker Session Chair: Dr. Chanel Tyler
9:30 am – 10:50 am	Faculty Talk: Dr. Colin Jefcoate and Panel Discussion Title " Endocrine Disruptors: Targets, Mechanisms and Risks" Location: Fluno Center Auditorium
10:50 am – 11:30 am	Trainee Talks Location: Fluno Center Auditorium Session Chairs: Carly Kibbe, Samantha Lewis
	10:50 – 11:10 am Yizhou Jiang
	11:10 – 11:30 am Dr. Heather Bankowski
11:30 am – 12:30 pm	Lunch – Fluno Center Dining Room
1:00 pm -2:00 pm	Keynote Speaker: Dr. Stephen Black Title " Regulation of NO Signaling by Oxidative and Nitrosative Stress " Session Chair: Dr. Ronald Magness
2:00 pm – 3:00 pm	Poster Session / Afternoon Break Location: Fluno Center Foyer
3:00 pm – 4:20 pm	Trainee Talks Session Chair: Brian Kenealy, Ann Rozner Location: Fluno Center Auditorium
	3:00 – 3:20 pm Kate Guerriero
	3:20 – 3:40 pm Omar Jobe
	3:40 – 4:00 pm Katie Hackbart
	4:00—4:20 pm Carly Kibbe
4:30 pm	Closing Remarks Location: Fluno Center Auditorium
4:30 pm	Poster take down

Keynote Speaker: Dr. Stephen Black

Dr. Stephen Black, PhD completed his B.Sc (honors) at the University of Edinburgh, Scotland in Molecular Biology and his PhD also from the University of Edinburgh, Scotland in Molecular Pharmacology. Dr. Black completed postdoctoral training in Molecular Endocrinology at the University of Edinburgh, Scotland and then at the University of California—San Francisco. Professional academic appointments at the University of California -San Francisco include Research Chemist, Laboratory Director of the Child Heath Research Center and Assistant Professor of Pediatrics through 1994. Dr. Black then moved to Northwestern University in Evanston, IL as an Associate Professor of Pediatrics and Molecular Pharmacology. Additional academic appointments at the University of Washington and University of Montana led to his current position as Professor of Obstetrics & Gynecology at the Medical College of Georgia. Research in Dr. Black's laboratory focuses on the roles of reactive oxygen species (ROS) in cell signaling and how derangements in ROS generation underlie many pathogenic states. Dr. Black has 150 PubMed publications and is active in numerous professional societies including Society for Pediatric Research, Society for Neuroscience and the American Heart Association.

Regulation of NO Signaling by Oxidative and Nitrosative Stress

Keynote Speaker Abstract – One of the major goals of my laboratory is to understand how nitric oxide (NO) signaling is regulated in the endothelium under both physiologic and pathologic conditions. To this end we have focused on how the endothelial isoform of NO synthase (eNOS) is regulated. I will discuss how we are attempting to integrate mass spectroscopy and molecular modeling into our cell biology studies to elucidate new mechanisms that regulate NO signaling by oxidative and nitrosative stress. I will focus on three main areas: control of eNOS dimerization, eNOS phosphorylation, and eNOS subcellular trafficking. Finally, I will discuss how our investigations into these more basic control pathways allowed us to develop a potential new therapy for the treatment of the endothelial dysfunction that precedes the development of pulmonary hypertension in children born with congenital heart defects that lead to increases in pulmonary blood flow after birth.

Dr. Colin Jefcoate, PhD
Professor, Pharmacology

Title Endocrine Disruptors: Targets, Mechanisms and Risks

A wide range of persistent environmental chemicals disrupt hormonal signaling pathways ,particularly those involving reproductive organs .These chemicals include many organochlorine compounds ,plastic components including BHA and phthalates and pesticides including atrazine,organophosphates and recently tributyl tin. These chemicals are commonly found in lakes rivers and ground water are readily enter the food chain .Their effects were first realized through developmental effects on wildlife . Many of these chemicals bind to the estrogen receptor thus the frequently reported wildlife feminization . Links through Public Health studies have been made to several diseases affecting male and female reproductive health including breast and prostate cancers . The accumulation of these chemicals in body fat and ready excretion through lactation poses additional risks to the fetus . The potential for imprinting adult effects in the fetus expands human risk beyond endocrine diseases . In assessing the human risks there have been extensive efforts to quantify exposures ,particularly in pregnant mothers and in children. Exposures to many of these chemicals appears to be in the range of receptor activity.

Recent work has expanded the mechanisms of disruption to several other nuclear receptors (PPAR ,RXR and SF-1) where these chemicals bind and compete with the natural hormone . The result is persistent activation or inhibition of the transcription of target genes that by-passes the normal tight hormonal controls.

Chronic Hypoxia Induces Differential Gene Expression In Human Umbilical Vein Endothelial Cells

Yi-zhou Jiang, Kai Wang, Ping Wang, Christina Kendziorski, Dong-bao Chen, and Jing Zheng

Endothelial cells in most tissues in vivo reside under chronic hypoxic environment (2-8% O2). This physiological hypoxia is critical for endothelial cell homeostasis, growth and development. To examine molecular mechanisms underlying chronic hypoxia regulation of human endothelial cell functions, herein we compared the transcriptomes of human umbilical cord vein endothelial cells (HUVEC) derived under hypoxia or normoxia. Methods: HUVEC were isolated from umbilical cords (n = 6) of normal term pregnancy and cultured under hypoxia (37o C, 5% CO2, 3% O2) or normoxia (37o C, 5% CO2, 95% air). After 20-25 days, the phenotypes of the cells were verified. Highly pure cell preparations (> 96% of cells expressing CD31 and exhibiting positive LDL uptake) were used. The transcriptomes were analyzed by using the Affymetrix human U133 plus 2.0 microarray chips. Results: Both hypoxia- and normoxia-derived HUVEC maintained typical endothelial cell phenotypes after 20-25 days of culture. Hypoxia-inducible factor 1 α (HIF1α) protein levels were significantly increased in hypoxia-derived HUVEC vs. normoxia-derived HUVEC. Microarray analysis revealed that chronic hypoxia induced 62 differentially expressed (DE) genes, in which 41 genes were up-regulated and 21 genes were down-regulated. Ten of genes were verified by RT-PCR. Among these 62 DE genes only 5 were overlapped with those previously reported in normoxia-derived HUVEC exposed to acute (12, 24, and 48 hr) hypoxia. The gene enrichment analysis showed that the majority (12.9 %) of these DE genes were critical for cell adhesion, while others were important for membrane organization and biogenesis (6.5%), cell activation (6.5%), and cell migration (6.5%), according to their functions in biological process. In addition, 11.3% of these DE gene products were located in mitochondria, many of which are known to be involved in energy metabolism. Conclusions: In HUVEC, chronic hypoxia induces a transcriptome significantly different from these under chronic normoxia and acute hypoxia. Thus, HUVEC developed under chronic hypoxia represents a novel endothelial cell model which might more closely mimic their in vivo environment. Chronic hypoxia induced clusters of DE genes mainly participating in cell adhesion and energy metabolism.

Striking Developmental Changes in Kisspeptin-Gpr54 Signaling to GnRH Nurons in Female Monkeys: Modification by Estrogen Feedback.

Guerriero KA, Keen KL, Terasawa E

A gonadal steroid-independent increase in GnRH release triggers the onset of puberty in primates. Because kisspeptin-Gpr54 signaling is important for the pubertal increase in GnRH release, in this study we examined how kisspeptin-Gpr54 signaling is regulated by ovarian steroid feedback in female rhesus monkeys. To assess the effects of ovariectomy (OVX) on developmental changes in kisspeptin-54 release pattern and the GnRH response to the kisspeptin agonist, human kisspeptin-10 (hKP10), we measured kisspeptin-54 and GnRH release in the stalk-median eminence of prepubertal and midpubertal monkeys using a microdialysis method. Results are summarized: 1) A developmental change in kisspeptin-54 release occurred at puberty, as seen by an increase in mean release and pulse frequency, but not pulse amplitude, 2) OVX stimulated mean kisspeptin-54 release and pulse amplitude in midpubertal, but not prepubertal, monkeys, 3) 10 nM hKP10 stimulated GnRH release similarly in both prepubertal and midpubertal ovary-intact monkeys, and 4) the GnRH response to hKP10 remained the same after OVX in prepubertal monkeys, whereas OVX eliminated the hKP10-induced GnRH stimulation in midpubertal monkeys. These results suggest that the pubertal increase in kisspeptin-54 release is independent from ovarian steroid feedback, and that kisspeptin-Gpr54 signaling to GnRH neurons undergoes a striking developmental change from an ovarian steroid feedback-independent to -dependent state. (Supported by NIH grants HD11355 and T32 HD041921).

Alterations in the Nitric Oxide Synthase (eNOS) Pathway of Human Umbilical Vein Endothelium of Normal and Diabetic Pregnancies

Heather A. Bankowski, Fu-Xian Yi, Ian M. Bird, Dinesh Shah

Diabetes mellitus (DM) is characterized by vascular dysfunction with variable effects on pregnancy and fetal growth. The possibility exists that human umbilical vein endothelial cells (HUVEC) of diabetic pregnancies may not undergo the vasodilation characteristic of normal pregnancy, which could thereby result in excessive or compromised fetal growth and associated pathology. The mechanism of this phenomenon is unclear but could result from altered eNOS activation and/or limited pool of active eNOS capable of nitric oxide (NO) production. Of particular interest is DM antedating pregnancy (pre-existing DM) that may produce unique endothelial dysfunction characteristic of a chronic disease state, and may also occur in the umbilical vasculature during months of development. This is the first translational investigation in humans which has sought to determine directly if there is a functional difference in eNOS activation between the HUVEC of non-diabetic pregnancies and in pregnancies with pre-existing DM. Methods of dual imaging of calcium [Ca2+] response to vasodilation and simultaneous NO production in uterine artery endothelium in HUVEC have been utilized to study the vasculature of normal and preeclamptic pregnancies. These same methods were recently used to determine endothelial dysfunction in diabetic pregnancies. Umbilical veins from the cords of normal (N=7) and diabetic (N=5) subjects (obtained with authorized consent) were imaged using Fura-2 and DAF-2 do detect Ca2+ and NO respectively in real time in response to stimulation with ATP (100 uM). Recordings show that [Ca2+] signaling in the HUVEC of diabetic pregnancies appears similar to that of normal pregnancy, with a clear initial peak followed by repeated Ca2+ bursts that are synchronized between cells. However, the sustained NO production that is characteristic of normal pregnancy is lacking in the diabetic HUVEC. This was also true in response to the pharmacologic stimulant ionomycin, suggesting this is a limitation at the level of eNOS activation, which contrasts prior findings in previous studies of the HUVEC of preeclamptic pregnancy, where endothelial dysfunction is evident as a failure to signal at the level of [Ca2+]. We conclude that while in diabetic pregnancies [Ca2+] signaling is normal, the difference between normal and diabetic pregnancies is due to decreased production of NO, occurring at the level of decreased activation of eNOS. Such a failure to respond is consistent with direct damage to eNOS by reactive oxygen species (ROS), toxic substances known to be perpetuated by the hyperglycemic environment of DM.

Pregnancy Specific Estradiol-17β-Mediated Proliferation in Uterine Artery Endothelial Cells: Role of ER-α vs. ER-β in Angiogenesis

Sheikh O. Jobe1, Jayanth Ramadoss1, Jill M. Koch1, Yizhou Jiang1,

Depts. of Ob/Gyn. Perinatal Research Laboratories, 2 Pediatrics and 3 Animal Sciences, University of Wisconsin-Madison.

Abstract: Pregnancy is associated with dramatic rises in uterine blood flow (UBF) which result from vascular adaptations including vasodilatation and angiogenesis. These adaptations are critical and are implicated directly in pathologic pregnancies such as preeclampsia and IUGR. Regulation of vasodilatation is mediated in part by estradiol-17β (E2β) through its classical receptors ER-α and ER-β. However, its role in uterine angiogenesis during gestation is less characterized. We hypothesized that E2β will cause greater angiogenic responses in uterine artery endothelial cells from pregnant ewes (P-UAECs) vs. cells from nonpregnant ewes (NP-UAECs) and that these responses will occur via ER-α and/or ER-β. Methods: P-UAECs (passage 4, day 120-130; term= 147 days; n=6) and NP-UAECs (passage 4, NP; luteal n= 5 and follicular n=2) were treated with vehicle (control, basal media) or increasing concentrations of E2β. In vitro index of angiogenesis was evaluated utilizing the BrdU Proliferation Assay technique following 16 hrs of serum starvation and 24 hrs of E2β treatment. Blockade of receptors was performed utilizing specific antagonists, ICI 182, 780 (ER-α/ER-β), or MPP dihydrochloride (ER-α), or PHTPP (ER-β). Whereas activation of ER-α- and/or ER-β was done utilizing specific agonists PPT (ER-α) or DPN (ER-β). Results: As hypothesized, E2β treatment significantly induced P-UAEC proliferation ($P < 0.05$) more than in NP-UAECs. Maximum mitogenic responses were seen at a physiologic E2β concentration of 0.1 nM (2.06 + 0.23 fold of control in P-UAECs vs. 1.27 ± 0.13 in NP-UAECs). ICI 182,780 and the ER-β antagonist PHTPP completely abrogated E2β-induced P-UAEC proliferative responses whereas MPP had no effect. Consistent with these data, as seen with E2β treatment, stimulation of ER-β with DPN significantly induced P-UAEC proliferation ($P<0.05$) and activation of ER-α with PPT had no effect. In combination, PPT and DPN did not stimulate an additive effect on P-UAEC proliferation. Conclusions: These data demonstrate the significance of E2β actions specifically via ER-β in uterine angiogenesis regulation during pregnancy. Selective responses of P-UAECs further illustrate estrogenic programming during pregnancy at the level of the uterine artery endothelium. NIH HL49210, HD38843, HL87144 and R25GM083252

Effect of Insulin Resistance on Follicle Development and Ovulation

Katherine S. Hackbart, Rudelle K. Meyer, Pauline M. Cunha, Robert W. Bender, Hemanta K. Shrestha, Patrick Kusilek, and Milo C. Wiltbank

Polycystic ovarian syndrome (PCOS) is a reproductive disorder affecting 1 in 5 women that is characterized by excessive androgen levels, anovulation, and polycystic ovaries. There also appears to be an association between PCOS and insulin resistance. In this work, we studied the effect of dexamethasone-induced insulin resistance on bovine follicle development and function as determined by ability to ovulate. EXPERIMENT 1: Cows were given Dexamethasone (15 mg, i.m.; T1; n=5) or saline (7.5 ml, i.m.; C1; n=4) once daily. At the initiation of treatment, an intravaginal progesterone-releasing device (CIDR) was inserted in all animals and rBST (500 mg, s.q.) was administered to T1 animals. One week later, the CIDR was removed and cows underwent follicular aspiration to remove follicles ≥5 mm to induce a new follicular wave. PGF2α (25 mg, i.m.) was also administered to induce luteal regression, and T1 cows received a second dose of rBST. Blood samples were collected once daily prior to feeding to determine glucose, insulin, and progesterone. Ovarian structures were measured once daily via transrectal ultrasound. Treatment significantly increased glucose (T1=105.0 mg/dl, C1=57.9 mg/dl; P<0.01) and insulin (T1=118.4 µU/ml, C1=19.1 µU/ml; P<0.01) concentrations. Treatment also abolished ovulation (T1=0/5; C1=4/4; P<0.01) and thereby decreased progesterone concentrations at days 12 (P=0.01), 14 (P<0.01), and 16 (P<0.01) after follicular aspiration. To reduce health concerns due to Dexamethasone administration, a preliminary study was then performed in which cows (n=3) were treated with a lower dose of Dexamethasone (10 mg, i.m.) once daily and no rBST was administered; a similar increase in glucose and insulin as well as a similar anovulatory phenotype were observed in all animals. EXPERIMENT 2: To test the hypothesis that treatment affected ovulation through LH signaling, cows (n=7) were utilized in a cross-over design experiment. Cows were given Dexamethasone (10 mg, i.m.; T2) or saline (5 ml, i.m.; C2) once daily. At the initiation of treatment, cows were administered PGF2α and a CIDR was inserted. Three days later, cows underwent follicular aspiration. Seven days after aspiration, the CIDR was removed and 6.5 hrs later cows were administered GnRH (200 µg, i.m.). Blood samples were collected once daily prior to feeding to determine glucose, insulin, and progesterone. E2 was measured daily beginning one day after aspiration until the day of the GnRH injection. Blood samples were also collected at 0, 1, 2, 3, and 4 hrs post-GnRH to measure LH. Animals underwent ovarian ultrasonography once daily. Treatment significantly increased glucose (T2=85.4 mg/dl, C2=57.5 mg/dl; P<0.01) and insulin (T2=88.2 µU/ml, C2=21.1 µU/ml; P<0.01) concentrations, but did not affect the production of an LH surge in response to exogenous GnRH (T2=7/7; C2=7/7), LH concentrations (P=0.735), ovulation in response to exogenous GnRH (T2=7/7; C2=7/7), or progesterone concentrations (P=0.329). Treatment decreased estradiol on days 6 (T2=1.47 pg/ml; C2=2.66 pg/ml; P<0.01) and 7 (T2=1.43 pg/ml; C2=3.05 pg/ml; P<0.01) after aspiration. EXPERIMENT 3: To test the hypothesis that treatment abolished ovulation by affecting the positive E2 feedback, cows (n=8) were utilized in a cross-over design similar to Experiment 2. Treatments consisted of Dexamethasone (10 mg, i.m.; T3) or saline (5 ml, i.m.; C3) once daily. Treatment and hormone administration were similar to Experiment 2 except that at 12 hrs after removal of the CIDR, cows were administered exogenous E2-17β (0.5 mg, i.m.). Blood samples were collected daily as in Experiment 2 to determine glucose, insulin, and progesterone, as well as at 0, 1, 2, 4, 6, 8, 10, 12, 14, 16, 18, and 20 hrs post-E2 injection to determine LH concentrations. Cows underwent ovarian ultrasonography once daily. Treatment significantly increased circulating glucose (T3=83.2 mg/dl, C3=54.9 mg/dl; P<0.01) and insulin (T3=100.0 µU/ml, C3=21.4 µU/ml; P<0.01) concentrations. Additionally, treatment abolished the E2-induced LH surge, or delayed it such that it was not observed in the time period during which blood samples were collected (T3=0/8; C3=8/8).

Treatment decreased ovulation (2/8) in response to exogenous E2. However, some T3 cows had a late ovulation (2/8; ovulation 4-7 d after E2, well past the physiologically relevant time in relation to exogenously administered E2). 4/8 T3 cows were anovular throughout the experimental period. C3 ovulation rate was 8/8. Treatment significantly decreased progesterone in T3 animals at days 5 ($P<0.01$), 7 ($P=0.02$) and 9 ($P=0.03$) after initiation of treatments. We conclude that treating cows with Dexamethasone significantly increases circulating glucose and insulin, decreases estradiol at days 6 and 7 of the follicular wave, and induces an anovular condition which is fully reversible by exogenous GnRH but only minimally reversible by exogenous estradiol.

FOXO1 Inhibits TXNIP Transcription in Pancreatic Beta Cells

Carly Kibbe, Ashley Schmitting, Hyunjoo Cha-Molstad and Anath Shalev

Thioredoxin-interacting protein (TXNIP) binds and inhibits thioredoxin, a redox regulator, resulting in increased cell apoptosis. Using mouse models, we recently found that TXNIP deficiency inhibits beta cell apoptosis and protects against type 1 and type 2 diabetes. These results suggest that TXNIP may be a possible target for therapies aimed to stop beta cell apoptosis in diabetic patients, however more must be known about the mechanisms regulating TXNIP. The forkhead box O1 transcription factor (FOXO1) has been shown to bind the TXNIP promoter and regulate the expression of TXNIP in different tissue types, but no data is available for pancreatic beta cells. Therefore, we first demonstrated that FOXO1 binds the TXNIP promoter in human islet cells, as assessed by Chromatin Immunoprecipitation (ChIP) assays. Using transient transfections of a FOXO1 expression plasmid we further showed that overexpression of FOXO1 in rat insulinoma (INS-1) cells significantly decreases endogenous TXNIP mRNA and protein levels. Using luciferase reporter assays we also demonstrated that FOXO1 overexpression reduces TXNIP promoter activity in INS-1 cells. However, a promoter deletion analysis revealed that rather than the known consensus FOXO1 binding site a downstream E-box was responsible for FOXO1 regulation of TXNIP. We have previously shown that glucose-induced TXNIP expression is mediated through carbohydrate response element-binding protein (ChREBP) binding to this E-box in the TXNIP promoter. In fact, using another set of luciferase reporter assays we demonstrated that FOXO1 overexpression blocks glucose-induced TXNIP expression. Furthermore, using ChIP assays we showed that FOXO1 overexpression leads to decreased ChREBP binding to the TXNIP promoter. Together, these results demonstrate for the first time that FOXO1 regulates TXNIP expression in pancreatic beta cells, and suggest that FOXO1 acts through ChREBP.

Chronic Treatment of Female Marmoset Monkeys with Serotonergic Analogues (+)-8-OH-DPAT or Flibanserin Differentially Alters Responsiveness of the Hypothalamic-Pituitary-Adrenal Axis to Restraint and Acute Serotonergic Challenge

Yves Aubert, Michael A Bohl, Jason R Lange, Amber K Edwards, Morgan L Gustison, Bernd Sommer, Kelly A Allers and David H Abbott

Stress-induced activation of the hypothalamic-pituitary-adrenal (HPA) axis is partly mediated by brain serotonin (5-HT) release. To examine how chronic administration of the 5-HT1a agonist R-(+)-8-hydroxy-2-(di-n-propylamino)tetralin (DPAT) and the 5-HT1a agonist/5-HT2a antagonist flibanserin (FLIB) affect the HPA axis in basal and challenged states, 8 adult female marmosets (Callithrix jacchus) housed in male-female pairs received daily subcutaneous (s.c.) injections of 0.1mg/kg DPAT or vehicle (VEH) for 10 wk in a cross-over design, while an additional 8 females received daily oral preparations of 15mg/kg FLIB or VEH for 10wk using the same paradigm. All females were ovariectomized. Four received estradiol replacement and 4 did not. Basal cortisol (CORT) levels were determined between 08:45h-09:15h at wk 0, 3 and 6 of treatment, while adrenocorticotropin (ACTH) and CORT levels were determined at (1) 0, 15, 30 and 210 min following a 30-min restraint test, and (2) 0, 15 and 180 min following a 0.1mg/kg DPAT or saline s.c. injection (5HT test). Restraint and 5HT tests were administered during 8-10 wk of treatment. The adrenal responsiveness index (ARI) was calculated as [CORT]/log[ACTH]. Basal CORT levels were unaffected by chronic DPAT and FLIB. Restraint elevated ACTH and CORT after 15-30 min in all groups. Restraint-induced ACTH elevations in DPAT and FLIB treated monkeys were greater than those induced by VEH at 15-30 min, while CORT remained elevated at 210 min in DPAT, but not in FLIB treated monkeys. DPAT increased ARI at 210 min, but not during the immediate response to restraint. FLIB, in contrast, diminished ARI during the entire restraint test. An acute 5HT test increased ACTH after 15min, and CORT and ARI after 180 min in all animals. FLIB reduced ACTH levels overall, while chronic DPAT was without effect in the 5HT test. While similarly-induced HPA effects of DPAT and FLIB, such as increased ACTH responses to restraint, are most likely triggered by chronic activation of similar 5-HT1a receptor populations, differential effects, including FLIB- but not DPAT-induced reductions in ACTH levels during the acute 5HT test, may be caused by chronic FLIB-induced inhibition of 5-HT2a receptors, and the differential binding of FLIB to pre- and postsynaptic 5-HT1a receptors. FLIB-induced decreases in HPA parameters may indicate drug-related diminution in stress responses. Funded by Boehringer-Ingelheim GmbH.

Characterizing Membrane Properties of Ovine Pregnant Uterine Artery Endothelial Cells (P-UAEC)

Roxanne Alvarez, Ian Bird & Bikash Pattnaik

Departments of OB-GYN and Pediatrics. UW-Madison.

During pregnancy uterine artery endothelial function is enhanced, including greater cell-cell communication and correspondingly enhanced Ca2+ influx in response to agonists. Both adaptations of Ca2+ signaling result in enhanced vasodilation. The purpose of this study is to characterize the contribution of potassium channel(s) to resting membrane potential as a means for pregnancy to alter Ca2+ influx via TRPC channels in uterine artery endothelial cells (UAEC). In previous studies we have shown that Ca2+ activated and delayed rectifier potassium channels contribute to endothelial cell functional physiology. We undertook this study in order to understand the specific changes in contribution of these signaling ion-channels during pregnancy to coordinate cell-cell communication. Methods: Whole-cell method of patch clamp electrophysiology was carried out on single voltage clamped passage 4 P-UAEC plated to 20% density. Cellular responses to voltage changes in 10 mV steps or ramp protocol from -150 mV to +50 mV were recorded while using a –60 mV holding potential. The pipette solution contained K-gluconate (100mM), KCl (30mM), HEPES (5mM), EGTA-KOH (5.5mM), CaCl2 (0.5mM), and Mg-ATP (4mM) at pH 7.2. The bath solution contained KCl (5mM), NaCl (135 mM), HEPES (10mM), glucose (10mM), CaCl2 (1.8mM), and MgCl2 (1mM) at pH 7.4. Results: Preliminary data show that the resting membrane potential of P-UAEC is –20 ± 2.3 mV (n=6). The membrane capacitance was determined to be 19 ± 6 pF with a resistance of 0.388 ± 0.134 GΩ. Conclusions: Our data suggests that isolated P-UAEC have potassium channels that produce outward-rectifying current and hyperpolarize the membrane. The results also show a smaller inward current at hyperpolarizing potential. Our future direction in research is to determine the molecular identity of these underlying potassium currents, the relationship to pregnancy enhanced TRPC3 activation, and further to move towards channel agonist and antagonist experiments in whole animals, so revealing the vascular function of these channels in vivo.

Differential Regulation of CX43 Phosphorylation and Inhibition of Cell Coupling in Uterine Artery Endothelial Cells.

Derek S. Boeldt, Mary A. Grummer, Ronald R. Magness, Fu-Xian Yi, Ian M. Bird

Pregnancy increases blood flow to the uterus to meet the needs of the growing fetus. In preeclampsia, increased flow to the fetus is not achieved and the fetus is at risk of growth retardation. We have shown pregnancy-induced reprogramming of [Ca2+]i signaling in uterine artery endothelium (UAEC) enhances production of nitric oxide, and this depends on enhanced connexin43 (Cx43) gap junction communication. ATP and vascular endothelial growth factor (VEGF) both activate eNOS and both mediate [Ca2+]i responses, but this is not a cooperative or additive process. Pretreatment of 'pregnant' UAEC (P-UAEC) with VEGF-165 reduces the sustained phase of a subsequent ATP [Ca2+]i response to levels equivalent to those observed in nonpregnant UAEC (NP-UAEC). Inhibition of Cx43 in active gap junctions is implicated as the target for VEGF since pretreatment of P-UAEC with the Cx43 mimetic peptide Gap27 to disrupt cell coupling yields similar inhibition. Cx43 phosphorylation by PKC and/or ERK-1/2 (positions S262, S368, S279/282, and Y265) has been implicated in decreased Cx43 function in a number of cells in response to VEGF or TPA. We have previously reported ERK-1/2 stimulation in UAEC in response to both VEGF and TPA, and TPA is also capable of exerting similar inhibitory effects as VEGF and Gap27 on ATP-induced [Ca2+]i response in P-UAEC. Significant phosphorylation of Cx43 is seen when UAEC are treated with TPA, and full reversal occurs when cells are pretreated with the MEK/ERK inhibitor U0126, yet inhibition of ATP-stimulated [Ca2+]i signaling in P-UAEC is only slightly recovered (81% of inhibition remains) by U0126 'rescue'. Thus, Cx43 phosphorylation does not functionally correlate with TPA inhibition of the ATP stimulated [Ca2+]i response. VEGF is also capable of Cx43 phosphorylation, which is reversed by U0126 treatment. It is unknown at this time whether reversal of Cx43 phosphorylation in response to VEGF will 'rescue' the associated inhibition of the ATP induced [Ca2+]i response. Other indirect factors may be responsible, such as controlling assembly or stability of functional Cx43 plaques with spatial arrangements that are necessary for proper function. Further experiments are now required to determine if this is the case.
Supported by NIH grants HL079020, HD38843 and HD041921.

Cross Talk Between Vitamin A and Cytochrome P4501b1 in Early Embryogenesis

Justin Bushkofsky, Colin Jefcoate

Cytochrome P4501b1 (Cyp1b1) is potently inhibited by many flavonoid compounds that are present in human diet. Recent work shows that Cyp1b1 surprisingly contributes to the conversion of vitamin A to retinoic acid in neural crest cell types during embryogenesis and also to neovascularization through affects on endothelial cells. In contrast to normal C57Bl/6j mice, Cyp1b1-/- dams which otherwise breed normally, fail to carry a litter through parturition when introduced to a vitamin A deficient (VAD) diet early in gestation (<gd 10.5). They successfully litter when the VAD diet is introduced later in gestation (>gd 10.5). In wild-type (WT) dams, VAD can be started throughout gestation, without effect on the number of offspring. There is evidence that Cyp1b1 contributes to retinoic acid synthesis in the neural crest due to Cyp1b1's recently found role in retinoic acid generation and the lack of any retinaldehyde dehydrogenases in the neural crest. This is also supported by our preliminary experiments where vitamin A deficiency and Cyp1b1 deficiency combine to prevent early embryogenesis. We suspect that embryos are being lost through the diminished availability of retinoic acid in absence of Cyp1b1. A second target of VAD and Cyp1b1 interaction is suggested by the finding that neonatal VAD causes wild-type pups to develop very little fat even with a very high fat diet. By contrast, diet induced obesity is unaffected by VAD started at weaning in these pups. Cyp1b1-/- mice, even with excess vitamin A, are also resistant to this diet induced obesity. Although not expressed in hepatocytes, the effect of Cyp1b1 is substantially targeted to liver fatty acid metabolism and to suppression of PPAR signaling with over 1600 liver genes being significantly changed in the vitamin A sufficient state. Experiments will define the windows of development and the extent of VAD associated with adiposity suppression and determine whether there are parallel increases in liver fatty acid metabolism. Secondly we will determine whether liver changes, including PPARs and Cyps are similar to those characterized for Cyp1b1 deficiency. The overall objective of the proposed research is to test the hypothesis that Cyp1b1 deficiency or inhibition by dietary flavonoids can combine with vitamin A deficiency to substantially impact the early embryo development and postnatal imprinting through cell type selective deficiencies in retinoic acid synthesis. Determining the levels of dietary vitamin A needed for theses effects is one goal. We envision that cells which use Cyp1b1 rather than retinaldehyde dehydrogenase (RalDH) forms will be most susceptible. Important features of this work include distinguishing maternal and embryo effects of VAD, characterization of embryo changes, identification of the active periods for disruption, establishing retinoid reversibility and actual sensitivity for vitamin A.

Characterization of Ion Channels of Ovarian Tumor Cells by Whole-Cell Patch Clamping

Nick Claussen1, Arvinder Kapur1, Manish S. Patankar1, Bikash Pattnaik2
Department of OB//Gyn (1); Department of Pediatrics (2)

Ovarian cancer is chemo-resistant. In vitro cultures reveal that while some cells die, others do not. This could be a result of the heterogeneity of tumor cell populations. Emerging research indicates that ovarian tumors have a common clonal origin but become polyclonal, with different clones at both early and late stages of genetic divergence acquiring the ability to progress to metastasis thus making them substantially more difficult to treat (Khalique L et al.). While these cells are from the same basic line, morphological differences contribute to the differing responses to chemo-therapeutic agents. Surface expression of receptors, proteins and ion channels are amongst the most obvious differences between populations. In one study published by Lee et al. in the American Journal of Cell Physiology (2008), a cation channel found on cisplatin sensitive KB epidermoid cells is not found on the cisplatin resistant KCP-4 cell line derived from the KB line. The conclusion of this paper indicates that this particular channel, IK1, mediates the cell's sensitivity to cisplatin. By using a whole cell patch clamp technique, we expect to discover changes in ion channels in ovarian cancer cells. By tracking changes within the cell line, we can target these aberrant changes and devise novel strategies to attack the tumor using channel-specific therapeutic agents. We have used SKOV-3 cells as our cancer cell model Preliminary data have shown SKOV-3 cells have an average capacitance of 23.74 pF and a resting membrane potential of -6.35mV (n=10). This negative resting membrane potential indicates the presence of functional potassium channels. Data to this point proves the whole cell patch clamp technique to be effective and informative. Future studies include 1.) the identification of specific channels through the use of calcium, sodium and potassium channel agonists and antagonists 2.) the effects of cisplatin and carbotaxol on ion conductance and 3.) the effects of multi-modal tumor management strategies incorporating currently used chemo-therapeutic agents in combination with ion channel-specific agents.

Title

Luca Clemente

A tumorigenic mutation of the epidermal growth factor receptor (EGFR) that results in a tandem kinase domain duplication (TKD-EGFR) has been described in glioblastoma multiforme biopsies and cell lines. To determine the molecular mechanisms of TKD-EGFR activation when expressed in cells as well as the contribution of each duplicated kinase domain to receptor phosphorylation, we transfected B82L mouse fibroblast cells devoid of endogenous EGFR with wild type (WT) or TKD receptor. The TKD-EGFR displayed chronically elevated basal autophosphorylation at five known phosphotyrosine sites. Kinase activity-deficient knockouts of the N-terminal or the C-terminal kinase domains generated TKD-EGFRs that recapitulate the autophosphorylation/localization patterns of constitutively activated receptor versus WT-like EGFR, respectively. Though surface-localized subsets of the TKD-EGFR retain ligand responsiveness, immunofluorescence analyses have revealed a substantial portion of the receptor resides in the cytosol in an activated state. Our investigation of the molecular activity of the TKD-EGFR yields evidence for a unique mechanism of constitutive activity and dual kinase domain activation. Current research seeks to quantify the activity of each kinase domain of this novel receptor and to understand the mechanisms responsible for its primarily intracellular localization.

The Transcriptomic Analysis of Imprinted Genes During Early Embryonic Development in Cattle

Ashley M. Driver, Ricky L. Monson, Hasan Khatib

Genomic imprinting, a phenomenoa causing silencing of a single parental allele, occurs in a subset of genes important for early embryonic development. Knockout and copy number manipulation experiments of imprinted genes have been shown to result in conditions such as embryonic growth retardation and low post-natal survival rates in mice. Therefore, investigation of these genes is critical to gain a better understanding of the genetic framework driving development. The objective of our study is to investigate the differential expression of imprinted genes in Day 8 blastocysts compared to degenerate embryos that were arrested at Day 5 of development. In order to accomplish this goal, we will utilize an in-vitro fertilization system in cattle established recently in our lab. Briefly, oocytes were collected, matured, and subsequently fertilized (marked as Day 0 of development). These putative zygotes were then cultured over an 8 day period where numerous developmental and morphological changes are occurring including (but not limited to) cellular divisions, compaction, and differentiation into the eventual Inner Cell Mass (ICM) and Trophectoderm of the blastocyst. Of interest to our lab is the period between compaction and differentiation (Day 5 to Day 8 of development) as alterations in differentiation capacity of the cells from totipotent blastomeres to pluripotent cells of the ICM suggests a series of critical gene transitions to mediate proper differentiation and growth. Total RNA was extracted from pooled samples of blastocysts and degenerate embryos for quantitative real-time PCR (qPCR) analysis. Preliminary transcriptomic data in our lab has established 67 differentially expressed transcripts (including one imprinted gene) between the two in-vitro produced embryo populations; 33 of which had greater than 2-fold expression providing candidate genes for further investigation. However, because of the limitations of the microarray chip to identify lowly-expressed transcripts and the limited availability of some gene probes, little information on the expression of imprinted genes was obtained. As such, in this study, we will utilize qPCR to compare expression of all known imprinted genes in cattle between these two embryo populations. We hypothesize that there is a differential expression of imprinted genes between degenerates and blastocysts providing candidates for further functional and association studies. Future experiments aim to validate results in an in-vivo embryo population in order to determine if significant transcriptomic differences are due to properties intrinsic to the embryo or to effects of the IVF procedures itself.

Placental Iron Transporters in Sheep Fetal Growth Retardatin and Uterine Growth Restriction

Jason M. Habeck B.S., Jill M. Koch, PhD, , Katie Meyer, B.S., Ronald R. Magness, Ph.D., Pamela J. Kling, M.D.

Background: Iron transport via the placental to the fetus is impaired in growth-restricted fetuses, resulting in low tissue iron levels. We utilized a sheep uterine restriction model to study the effects of insufficient uterine space on placental and fetal development. Sheep and human placentae differ in tissue arrangement, with a single trophoblast layer in human, but both fetal and maternal trophoblast layers in sheep. It is known that cell surface transferrin receptor (TfR) is likely involved in human placental iron transport, but it is not known if TfR is involved in sheep placental iron transport. Hypothesis: TfR expression will increase in growth restriction due to the overcompensation of TfR transcription in response to low iron stores. Methods: To promote uterine restriction, ewes underwent a single uterine horn ligation 2 months prior to conception. Singletons, twins and triplets were delivered at 120 or 130 days gestation (term=145) under anesthesia. Controls included ligated and nonligated singletons, and nonligated twins. Uterine restriction included ligated twins, nonligated triplets, ligated triplets and nonligated quads. Placental weight, placentome number and types (A, B, C, D) were recorded. Placentomes were fixed in formalin, paraffin-blocked and tissues stained in H&E, Gomori Trichrome (collagen I) and Perl's Prussian Blue (hemosiderin iron). Additional tissues underwent antigen extraction and stained for CD-71 TfR. Digital photomicrographs were taken. Results: Microscopic placentome structures (vessels, microvessels, myometrium, endometrial glands, fetomaternal interface, and fetal chorion) were seen. Prussian blue iron stain showed minimal staining, except for small sites of very intense staining in a subchorial distribution in the hemophagic zone. Trichrome staining (collagen I) was seen mostly in the blood vessel wall supporting structure. In the uterine restricted group, additional collagen staining was observed outside the vasculature that could indicate tissue scar. Placentomes showed specific TfR staining in the intercotyledonary trophoblasts, endometrial glands, vascular endothelium, vascular smooth muscle, trophoblast cells at the junction of the villi, as well as on Hofbauer cells, with strongest staining on the intercotyledonary trophoblasts and weaker staining on the trophoblast cells. Placentae from the uterine restricted fetuses exhibited stronger staining of trophoblasts, endothelial, vascular smooth muscle and vascular support stroma, compared to the controls. Conclusions: Human TfR antibody binds specifically to sheep placenta. Greater collagen and TfR staining was observed in placentae from the uterine restricted fetuses, compared to control. These data support the hypothesis that TfR is involved in ovine fetal iron transport and TfR is upregulated in uterine restricted placentae.

Setting the Stage for Newborn Iron Deficiency

S.S. Hirschfield, B.A. Fischer, V. Sridhar, S.E. Blohowiak, C.L. Coe, P.J. Kling

Background: The antecedents of may illnesses and health vulnerabilities begin in infancy, and often before birth. One common concern in young infants is iron deficiency. Despite U.S. public health efforts to reduce iron deficiency, iron deficiency continues to affect 8-24% of infants in the US. Research has shown that maternal stress experienced during pregnancy may predispose the fetus to a number of health vulnerabilities that may set the stage for postnatal illness. Animal work shows that pregnancy stress may predispose to iron fetal iron deficiency. Thus, the purpose of the present study was to examine the impact maternal stress during pregnancy on newborn iron status. Methods: 165 mothers and their term babies (92 males; 73 females) were recruited from the Meriter Hospital Birthing Center in Madison, WI, prior to hospital discharge. At birth, a sample of each infant's umbilical cord blood was collected upon consent and subsequently processed to examine iron status markers. We examined whole cord blood and reticulocyte-enriched Zinc Protoporphryin/ Heme (ZnPP/H). Enriched ZnPP/H was measured after separating the youngest red cells. All enrolled mothers were asked to fill out a 35-item, retrospective questionnaire to assess the stress they had experienced during their pregnancy. The questionnaire prompted the mother to respond whether or not a particular stressful event had occurred during her pregnancy and to rate the stress impact of the item on a scale of 1-10 (1=did not upset me, 10=extremely disturbed). Results: Stress measure total score: M= 46.1; SD=40.5; total score range: 0-201. Stress measure mean: M=1.3; SD=1.2; mean score range: 0-5.74 suggesting that our sample experienced relatively low levels of stress during pregnancy. Despite reporting low levels of stress during pregnancy, hierachical linear regression analyses indicated that above and beyond maternal ethnicity, diabetes, anemia, and age, higher mean scores on the maternal stress measure ($\beta = .28$, $p<.001$) predicted higher enriched ZnPP/H ($F_{1,164}=3.6$; $p<.01$). In addition, after adding the 3 most stressful items into the overall regression model mean stress scores continued to predict newborn enriched ZnPP/H ($F_{1,164}=3.4$; $p<.01$) with mean stress scores accounting for 13.4% of the variance in enriched ZnPP/H. Conclusion: High maternal stress is predictive of high reticulocyte-enriched ZnPP/H, suggesting that maternal stress during pregnancy may impair late pregnancy iron delivery to the red cell.

Immune Cell-ovarian Tumor Cell Adhesion Through MUC16 and Immunocytokine.

Sachi Horibata, Jennifer AA Gubbels, Jennifer A Belisle, Paul M Sondel, Joseph P Connor, Manish S Patankar

Natural killer (NK) cells are immune cell types that function normally to eliminate tumor cells by forming an immune synapse. However, we have shown that the presence of mucin, MUC16, on the surface of epithelial ovarian tumor cells inhibits the function of NK cells in two ways: 1) steric barrier 2) inducing inhibitory signaling through Siglec-9. To increase recognition of tumors by NK cells, we utilized the immunocytokine, KSIL-2, which activates NK cells through IL-2 and mediates ADCC via the KS antibody. Using a plate adhesion assay, we demonstrate that KSIL-2 mediates increased NK-tumor cell interactions. Our data shows that KSIL-2 can overcome the immune evasion mediated by the large MUC16 molecule.

Anti Proliferative Effect of Conjugated Linoleic Acid on Ovarian Cancer Cell Lines

Arvinder K Kapur, Kai Ludwig, Mildred Felder, Mark Cook, Manish Patankar

Introduction: Conjugated Linoleic acid (CLA) is an unsaturated derivative of Linoleic acid, abundantly present in dairy products and meat. Several reports in literature suggest that fat and fatty acid promote tumor growth in animals; in contrast Linoleic acid has been shown to have anti carcinogenic activity both in vivo and in vitro likely because of its ability to inhibit Cox-2. By inhibiting Cox-2, CLA is also likely to activate Natural killer (NK) cell and cytotoxic T cell mediated anti-tumor immunity. In the current study, we investigate the effects of CLA on the proliferation of ovarian tumors and on its ability to enhance the anti-tumor cytotoxicity of NK cells. Methodology: Bioactivities of two CLA isomers, C9T11 and T10C12, were determined. Ovarian cancer cell lines CaOV-3, OVCAR-3 and SKOV-3 were plated in 96 well plates. The cells were treated with either Vehicle (Ethanol), CLA 25mm, 50mm and 100mm or 7mm Cisplatin with CLA 25mm, 50mm, 100mm for 24, 48 and 72 hr. At the end of incubation period proliferation was determined by MTT assay. Effects of CLA on the expression of MHC class I on the ovarian tumor cell lines was determined by flow cytometry. Results. Our preliminary results indicate that CLA (T10C12) isomer inhibited the growth of all three cell lines in dose dependent manner. However CLA (C9T11) isomer had no significant effect. CLA treatment in combination with Cisplatin had no additive effect on inhibition of cell proliferation. The flow cytometric analysis of the three cell lines for MHC class I expression showed that CaOV-3 cell line had the highest inherent expression of MHC class I followed by SKOV-3 and OVCAR-3. Treatment with CLA (C9T11 and T10C12) decreased the expression of HLA in CaOV-3 whereas only a partial reduction was observed with SKOV-3. No change in expression of MHC class I antigens was observed in OVCAR-3 cells following treatment with the CLA isomers Conclusion: CLA has anti-proliferative effect on ovarian cancer cell lines. The T10C12 isomer of CLA had a better effect than C9T11 isomer indicating a high degree of molecular specificity. MHC class I antigens protect tumor cells from NK cell attack. The ability of CLA to attenuate the expression of MHC class I molecules on at least a subset of ovarian cancer cell lines may suggest that this lipid may potentially be utilized to enhance NK cell-mediated anti-tumor immunity. Effect of Chronic Binge Alcohol on NO regulation and the Profile of NO-Related Caveolar Proteins in Ovine Pregnant Uterine Endothelial Cells

Involvement of Mitogen Activated Protein Kinase (MAPK) in Rapid Estrogen Action Mediated by GPR30 in Luteinizing Hormone Releasing Hormone (LHRH) Neurons.

Brian P. Kenealy, Kim L. Keen, and Ei Terasawa

Previously, we reported that 17ß-estradiol (E2) induces a rapid action in LHRH neurons. Moreover, this action is in part mediated through the G-protein coupled receptor, GPR30, as the GPR30 agonist, G1, caused an effect similar to E2 and transfection with GPR30 siRNA abrogated E2-induced changes in intracellular calcium ([Ca2+]i) oscillations (Noel et al., Mol Endocrinol 23:349, 2009). However, the mechanism of E2 action leading to [Ca2+]i oscillations and subsequent LHRH neurosecretion is still unclear. In the present study, first we re-examined the role of GPR30 in E2-induced [Ca2+]i oscillations using a novel GPR30 antagonist, G15, which recently became available. Second, we investigated the role of the mitogen activated protein kinase (MAPK) signaling in E2 rapid action, as the E2 action through GPR30 involves the MAPK system in cancer cells (Filardo et al., Mol Endocrinol 16:70-84, 2002). First, we confirmed that rapid E2 action in GT1-7 cells was mediated by GPR30, as G15 blocked the E2-induced [Ca2+]i oscillations. In the initial phase of the second study, we assessed the time course of rapid E2 action on mitogen activated protein kinase (MAPK). To our surprise, E2 increased phosphorylated ERK1 and 2 proteins within a minute of its application. Subsequently, the effects of the MEK inhibitor U0126 on the E2-induced [Ca2+]i oscillations were examined. The results in primate LHRH neurons indicate that U0126 did not interfere with the rapid E2-induced increase in the frequency of [Ca2+]i oscillations, indicating that the MAPK cascade appears not to be an upstream mediator of [Ca2+]i oscillations. The results are interpreted to mean that E2 rapidly phosphorylates ERK1 and 2 within a minute. Although we previously observed that E2 causes changes in [Ca2+]i oscillations and electrical firing activity, the finding showing E2 action on ERK1 and 2 phosphorylation within a minute is significantly faster than previous reports by other laboratories. Nonetheless, failure to block the E2-induced [Ca2+]i oscillations with U0126 in primate LHRH neurons suggests that the MAPK signaling appears not to be an upstream signal for the changes in [Ca2+]i oscillations. Whether signaling mechanisms, such as cyclic AMP and/or inositol(1,4,5) phosphate, are involved in the rapid action of E2 remain to be investigated.

Regulation of Steroidogenic Acute Regulatory (stAR) Gene By Protein Kinase A (PKA) and Salt Inducible Kinase (SIK)

Jinwoo Lee and Colin Jefcoate

StAR (Steroidogenic Acute Regulartory) protein when controlled by ACTH (adrenocorticotropic hormone) functions through increases in cAMP and activation of protein kinase A (PKA), which mediates the process by phosphorylation of CREB (cAMP Response Element Binding). There is a new kinase in adrenal cells, SIK (Salt Inducible Kinase) that functions by inhibiting the transcription of steroidogenic genes. SIK normally represses TORC (Transducer Of Regulated CREB), a nuclear factor that greatly enhances the CREB activity, by stabilizing the interaction with CBP (Creb Binding Protein), which has acetyl transferase activity. To characterize the binding of p-Pol II, p-CREB, TORC, SF1 (Steroidogenic Factor 1), CBP, Histone H3 and H4, I have used ChIP (chromatin immunoprecipitation) in relation to increases in primary transcript of Star, which has not undergone any modification after its synthesis. 8-Br-cAMP (0.4mM) and staurosporine (5~30nM) were used as a direct inhibitor of SIK. Surprisingly, staurosproine directly inhibits SIK and can replace cAMP analogs as a stimulant of StAR transcription. However, ChIP analysis revealed that these two treatments caused similar patterns in TORC2, CBP and CREB binding at 60min, but is significantly different in p-CREB, acetylation of Histone H3 and H4. Recruitment of SF-1, followed by phosphorylation of CREB and acetylation of Histone H3 and H4 sequentially occurred throughout the 1h time period after 8-Br-cAMP treatment but not with staurosporine treatment. This suggests that PKA mediated phosphorylation of CREB is not necessary for the TORC/CBP activation of transcription. Endoribonuclease-prepared siRNAs targeted to TORC2, SF1 and SIK are being developed to define their involvement.

Developing Models to Study Hedgehog Induced Steroidogenic Factor 1 Expression and Steroidogenesis

S.R.Lewis, J.S. Jorgensen

Disorders of sex development occur once in every 1500 live births and abnormal steroidogenesis during fetal development is often an important factor in producing these disorders. Steroidogenic Factor 1 (SF1) is required for steroidogenesis in many tissues where it has been shown to stimulate the expression of steroidogenic enzymes. In contrast to androgen synthesis in the adult Leydig cells, which relies on an intact hypothalamic-pituitary-gonadal axis to induce steroidogenesis, the fetal testis produces androgens in the absence of external endocrine signaling. Instead, hedgehog ligand (Hh) released by Sertoli cells signals in a paracrine fashion to fetal Leydig cells (FLCs), the steroid producing cells of the fetal testis. This Hh signaling up -regulates SF1 and subsequently induces the onset of androgen synthesis. The importance of the interaction between Hh and SF1 in fetal testis steroidogenesis has been suggested, but the molecular mechanism by which this interaction occurs has not yet been determined. We hypothesize that Hh signals are mediated through Sf1 to induce steroidogenesis and cell survival. A major barrier to testing our hypothesis is the lack of a model system in which to perform detailed molecular and biochemical studies of the link between Hh, Sf1, and androgen synthesis. Recently, it was discovered that advanced prostate cancer cells exhibit high Hh activity and synthesize androgens de novo. Therefore, we reason that just like in fetal testes, some prostate cancer cells use local Hh signaling to induce Sf1 expression and thereby, androgen synthesis, to support their survival. We have utilized both fetal testis and prostate cancer models to uncover the mechanism of Hh-induced Sf1 up-regulation and initiation of androgen synthesis. By using qRT-PCR we have determined SF1 is present in prostate cell lines that can produce their own androgens and have high Hh activity. In contrast, SF1 is absent in prostate cell lines that lack these attributes. In addition, SF1 was detected by immunohistochemistry in human advanced prostate cancer specimens, but not in benign prostate hyperplasia (which do not produce androgens). The presence of SF1 in these tissues and cell lines along with Hh activity suggests advanced prostate cancer may represent a useful model in which to study fetal steroidogenesis. Additional experiments are underway to characterize SF1 activity in prostate cancer cell lines to further understanding of Hh-mediated up-regulation of SF1 and the onset of steroidogenesis. These experiments will allow us to increase our knowledge of the role of this specific mechanism of fetal androgen synthesis both in normal function in the fetal testis as well as in deadly prostate cancer.

Zinc Protoporphryin/Heme Ratios (Znpp/H) as a Potential Newborn Screen for Iron Deficiency (ID)

S. L. Marmer, M. E. Chen, B. A. Fischer, V. Sridhar, S. E. Blohowiak, P. J. Kling

Background: Iron deficiency (ID), a common nutrient deficiency, impairs brain development. Newborn screening for ID has advantages, as earlier recognition of at-risk children could prevent long-term neurocognitive morbitity. ZnPP/H is an available, cost effective and sensitive biomarker of incomplete iron incorporation into erythrocytes. ZnPP/H, a potential candidate for newborn screening for iron deficiency, is measurable on whole cord blood or filter paper spots. Previous studies rinsed cord blood samples to remove pigments including bilirubin, that interfere with readings. Filter paper newborn screen samples cannot be rinsed and are obtained at 24-48 hrs after birth, when bilirubin levels may be elevated. Our aims were first, to examine the reproducibility of filter paper ZnPP/H measurements and second, to examine methods to limit bilirubin interference with ZnPP/H. Methods: We measured reproducibility of cord blood ZnPP/H eluted as hemolyzed blood from filter paper blood spots and whether eluted values correlated to the same whole blood samples. We measured the degree of bilirubin interference with ZnPP/H readings. We evaluated potential candidates to remove bilirubin interference with ZnPP/H, including detergents, albumin, and bilirubin oxidase. Results: Filter paper ZnPP/H was reproducible. Filter ZnPP/H correlated to whole or rinsed cord blood, P<0.0001, but lines of identity did not pass through zero. Although 5 mg/dL levels of bilirubin were similar to ZnPP/H without bilirubin, 10, 15 and 20 mg/dL increased the levels of ZnPP/H in a dose response fashion (P<0.0001). Tween 20 and Triton X-100 increased ZnPP/H baseline variability and did not remove bilirubin interference. Albumin decreased baseline ZnPP/H values to those of rinsed whole blood, but did not remove bilirubin interference. Bilirubin oxidase reagent is inexpensive and stable when refrigerated or frozen in water. Although not returned to baseline, bilirubin oxidase removes bilirubin interference by 70% (p<0.0001). Conclusion: Filter paper ZnPP/H correlated to intact whole and rinsed ZnPP/H, but bilirubin levels of 10 mg/dL interfere with readings. Bilirubin oxidase removes most bilirubin interference, improving the accuracy of filter paper ZnPP/H. Further studies are needed to validate the use of ZnPP/H from blood on filter paper.

Development of a Maternal Uterine Space Restriction Model in Sheep

Katie M. Meyer, Jill M. Koch, Jayanth Ramadoss, Pamela J. Kling, Ronald R. Magness

Asymmetric IUGR, associated with uterine anomalies and multi-fetal pregnancies, has been shown to cause asymmetric fetal body and organ growth as well as a multitude of adult diseases. In order to study the impact of human IUGR on the fetus, we developed an ovine uterine space restriction model. Multiparous ewes underwent a unilateral tubal ligation with intercorneal connections removed 2 months prior to breeding. Fetuses were delivered via c-section at 120d and 130d gestation (term 147d). Fetuses were studied in 7 groups: control singletons, twins, triplets and quadruplets (n= 9, 7, 7, 1), and unilateral singletons, twins, and triplets (n= 13, 6, 2). Placentome number and wt and body/organ measurements were recorded. Fetal artery creatinine and BUN as well as maternal artery and fetal vein glucose, triglycerides, and cholesterol were measured.Total placentome # /fetus showed clear demarcation with control singletons, unilateral singletons, and contro l twins having more placentomes/fetus than unilateral twins, control triplets, unilateral triplets, and control quadruplets (P<0.003), with 2 distinct groups defined: non-restricted restricted. Fetal plasma creatinine and BUN levels are determined by placental function and were 25% and 13% higher in restricted fetuses at 130d (P<0.05) Restricted fetuses had lower fetal weight, abdominal girth, thoracic girth, and crown-rump, at 130d, but not at 120d. BMI, head width, head length, and brain weight were similar at both time points in both groups. USR negatively altered heart, kidney, liver, spleen, adrenal, and thymus weights. Asymmetrical organ growth, as noted by decreased fetal and organ measurements, high creatinine and blood urea nitrogen, and increased maternal artery umbilical vein ratio of glucose, triglycerides, and cholesterol, is seen by 130 days gestation. This model is a tool to further study how fetal growth restriction alters fetal in utero development.

Rapid Changes in Bone Mineral Balance in Response to Estrogen Depletion in Rhesus Monkeys Detected Using a Tracer-less Calcium Stable Isotope Technique

JL Morgan jlmorga3@asu.edu1, DH Abbott, PhD, abbott@primate.wisc.edu2,3, A Anbar, PhD, anbar@asu.edu1,4, G Gordon, PhD, gwyneth.Gordon@asu.edu4, JL Skulan, PhD, jlskulan@geology.wisc.edu5 and RJ Colman, PhD, rcolman@primate.wisc.edu2. 1Department of Chemistry and Biochemistry, Arizona State University, Tempe, AZ, United States, 85287; 2Wisconsin National Primate Research Center, University of Wisconsin, Madison, WI, United States, 53715; 3Department of Obstetrics and Gynecology, University of Wisconsin, Madison, WI, United States, 53792; 4School of Earth and Space Exploration, Arizona State University, Tempe, AZ, United States, 85287 and 5Geology Museum, University of Wisconsin, Madison, WI, United States, 53706.

Significance: Understanding of bone metabolism and therapeutic development are hampered by an inability to detect rapid changes in bone mineral balance (BMB) or bone mineral density. Conventional biochemical markers provide information on relatively short-term changes in bone formation and resorption separately, but they reflect bone remodeling rate not precise quantifiable changes in BMB. By contrast, the natural Ca isotopic composition of soft tissue and urine directly reflects BMB, not remodeling rate. High-precision measurements of changes in the natural Ca isotopic composition of urine reflect changes in BMB after four weeks of bed rest in humans(1). Here we test the ability of Ca isotopic analysis to detect changes in BMB within 2 weeks of estrogen -depletion bone loss using a well-developed nonhuman primate model, the female rhesus monkey.

Study design: Six adult (12-16 years) female rhesus monkeys were randomized to control (C, n=3) or treatment (MPA, n=3) groups. Animals in the MPA group received an intramuscular (i.m.) injection of 150 mg of medroxyprogesterone acetate (MPA, a known suppressor of ovarian estrogen lasting 30 days/dose) on days 0, 28 and 56. At the same timepoints, C animals were given volume-matched saline i.m. Urine was collected for Ca isotopic analysis on days -7,-1,0,1,2,4,6,7,8 and 14. Ca analyses were done by inductively coupled plasma mass spectrometry (Neptune ICP-MS, Thermo Scientific, Waltham, MA). Conventional bone biochemical markers and circulating estradiol levels also were measured.

Results: Ca isotopes revealed a more negative BMB in MPA compared to C females from an increased negative slope (p<0.05) in Ca isotope ratios between baseline (day -7) and treatment period (days 1-14; C:-0.011 0.012, MPA:-0.046 0.018). All values were adjusted for age as baseline Ca isotope ratios were inversely correlated with age (r2=0.87, p<0.01), indicating naturally occurring increased bone mineral loss in older animals. Compared to baseline, estrogen was decreased (p<0.05) and osteocalcin and NTx levels were unchanged in MPA females.

Conclusion: Mass spectrographic measurements of urinary Ca reveal loss of bone Ca within a week of onset of estrogen depletion in adult female rhesus monkeys while traditional markers of bone turnover did not change. Such sensitive and rapid detection of bone mineral loss promises new insight into understanding short-term dynamics in bone metabolism.

References: (1) Skulan J, et al Clin Chem 2007; 53:1155-1158

Sources of Support: Supported by: NASA Grant Number NNX08AQ36G award to AA at Arizona State University; UW Institute for Clinical and Translational Research award to RJC (funded through NIH/NCRR Clinical and Translational Science Award 1UL1RR025011 to the University of Wisconsin, Madison); grant P51 RR000167 to the Wisconsin National Primate Research Center, University of Wisconsin, Madison; this research was conducted in part at a facility constructed with support from Research Facilities Improvement Program grant numbers RR15459-01 and RR020141-01.

Differential Programming of Gap Junction Connexin Proteins 43 and 37 in Ovine Uterine Artery Endothelium

Timothy J. Morschauser, Jayanth Ramadoss, Jill M. Koch, Gladys E. Lopez, Ian M. Bird, Ronald R. Magness

INTRODUCTION: Synchronized and sufficient uterine vascular endothelial adaptations facilitate the dramatic increase in uterine blood flow during pregnancy. These adaptations are thought to be modulated by the coordinated interaction between intercellular gap junction proteins and eNOS activation. HYPOTHESES: We hypothesized that expression of the gap junction proteins connexin (cx) 43 and 37 in uterine artery endothelium (UA endo) is elevated during pregnancy compared to nonpregnant luteal and follicular phases. We further hypothesized that restricting pregnancy to a single uterine horn will show a unilateral increase of connexin expressions only in UA endo from the gravid horn. METHODS: Restricting pregnancy to a single uterine horn (gravid unilateral) was established by surgically severing the vascular intercorneal connections and then ligating one horn (i.e. contralateral nongravid unilateral) 3-4 weeks before breeding. UA endo were isolated from nonpregnant sheep [luteal (n=4 vessels) and follicular (n=4)] and pregnant sheep [nongravid unilateral side (n=2), gravid unilateral side (n=2), and control pregnant (n=3)]. cx43 and cx37 protein expression was determined by Western analysis. RESULTS: Immunoblotting demonstrated that both cx43 and cx37 were significantly elevated in pregnant UAendo compared to luteal ($P<0.001$), follicular ($P<0.001$), nongravid unilateral ($P<0.001$) and gravid unilateral (cx43, $P=0.022$; cx37, $P<0.001$) UAendo. No difference was observed between luteal and follicular cx43 and cx37 expression in UA endo. Additionally, cx43 expression was significantly elevated in the gravid unilateral horn compared to the nongravid horn ($P=0.045$). In contrast, this difference was not observed in cx37 as it was barely detectable in both the nongravid and gravid horns. CONCLUSIONS: These data demonstrate that there is a distinct difference in uterine vascular programming of gap junction proteins cx43 and cx37 during pregnancy. Both cx43 and cx37 are lower in unilateral gravid compared to pregnant, suggesting that fetal restriction to a single horn has a direct effect on connexin expression during pregnancy. These data suggest that the regulatory mechanisms pertaining to gap junction proteins may delineate a greater understanding of vascular adaptations during pregnancy. However, further functional studies are still needed to fully understand these adaptations. NIH HL49210, HD38843, HL87144.

Modeling Pancreas Development in Embryonic Stem Cells by Ectopic Expression of Pancreatic Transcription Factor 1a (PTF1A)

Gopika G Nair, Robert Vincent, Nathan Treff, Jon S Odorico

Pancreatic development in mammals is controlled, in part, by the temporal expression of numerous genes that encode transcription factors. Yet, how these factors regulate each other and their target genes is not completely understood. Pancreas-specific transcription factor 1a (ptf1a) is known be to be involved in pancreas specification in the foregut endoderm and transactivation of the PDX1 promoter. A tetracycline-inducible murine ES cell line with temporally-controlled induction of ptf1a (tet-ptf1a) was established, which we utilized as a new tool to interrogate the role of PTF1a in directing differentiation of ES cells down the pancreatic lineage. Induction of ptf1a expression by doxycycline (Dox) treatment in differentiating ES cell cultures resulted in extensive expression of PDX1, consistent with PTF1a's known ability to transactivate the PDX1 promoter. In particular, the EBs gave rise to PTF1a+PDX1+ bud-like structures reminiscent of in vivo pancreatic organogenesis, in that cells of the differentiating PDX1+ epithelium expressed other pancreatic markers, such as carboxypeptidase A1 (CPA1) and neurogenin 3 (NGN3), and became progressively post-mitotic with time. The expression of amylase and islet endocrine hormones at later time points indicated that these cells were capable of further differentiation into mature pancreatic cell types. To understand the dosage dependent effects of PTF1a in directing differentiation into endocrine cells, we induced the tet-ptf1a cell line with different concentrations of Dox. The tet-ptf1a cell line is highly conducive to these experiments showing a direct correlation between the concentration of Dox and induced PTF1a expression levels. At low levels of PTF1a we observed increased numbers of Ngn3+ Pdx1+ endocrine progenitor cells compared to the number of like cells at high levels of PTF1a. On further differentiation, low dose PTF1a cultures exhibited the highest number of insulin and PDX1 co-expressing cells. We then interrogated the transcript levels of Rbpj and Rbpj-l, mammalian Suppressor of Hairless paralogs, whose gene products bind similar promoter sequences and the PTF1a protein. Upon induction of PTF1a expression in ESCs, transcript levels of Rbpj-l increased from very low levels initially to high levels, while Rbpj was constitutively expressed regardless of PTF1a expression and remained constant through a differentiation time course. Furthermore, amylase expression was significantly higher at high doses of Dox or PTF1a induction. That Ngn3+ and insulin+ endocrine cells were more prevalent at low induced levels of PTF1a, and amylase and Rbpj-l expression was greater at high doses of PTF1a induction indicates that the intracellular level of PTF1a controls the switch between exocrine and endocrine fates in our ESC-derived pancreatic progenitors. Prior embryonic pancreas tissue studies showed that initially RBPJ is bound to PTF1a early in development, and that this complex binds the promoters of Rbpj-l and other exocrine genes, and as development progresses, RBPJ-L accumulates due to transactivation by PTF1a and displaces RBPJ leading to exocrine development. Hence, as in pancreatic tissue studies, our data in ESCs suggests PTF1a and its DNA binding partners regulate endocrine vs. exocrine fate during pancreas development. Furthermore, this is the first study to show branching morphogenesis with both acinar and islet formation similar to in vivo pancreatic development in ES cell derived cultures.

Heparin Effect on Proliferation and Chemosensitivity of Ovarian Cancer Cells

Nonyem A. Onujiogu, Arvinder K. Kapur, Mildred Felder, Joseph P. Connor

Introduction: Heparin is a negatively charged, highly sulfated glycosaminoglycan. Ovarian cancer patients are frequently treated with heparin, as an anticoagulant, either prophylactically during their post operative hospitalization or therapeutically when they have been diagnosed with a blood clot. Heparin has been reported to have both anti-proliferative and mitogenic effects on some cancer cell lines. Hypothesis: We hypothesize that heparin is associated with an increased proliferation rate of ovarian cancer cells and that this change will alter the chemo-responsiveness of ovarian cancer cell lines SKOV3 and OVCAR3. Methods: We cultured ovarian cancer cell lines, SKOV3 and OVCAR3. These cells were treated with heparin for three months at a concentration of 50units/mL. Tritiated thymidine assays were used to estimate the role of proliferation in both heparin treated cell lines and control cell lines. Methylthiazol Tetrazolium Assay was used to asses the percent of live cells after treatment of the heparin treated and control cell lines with cisplatin. Results: In the tritiated thymidine assay, heparin treated OVCAR3 cells incorporated up to 75% more thymidine than the control OVCAR3 cells. SKOV3 cells had an opposite response to heparin. The heparin treated SKOV3 cells incorporated 50% less thymidine than the control SKOV3 cells. Heparin treated OVCAR3 cells had on average 20% more live cells at every concentration of cisplatin treatment when compared to control OVCAR3 cells. The opposite response was seen in SKOV3 cells. Heparin treated SKOV3 cells had on average 10% less live cells compared to control SKOV3 cells when treated with cisplatin. Conclusion: Heparin results in increased proliferation and decreased cisplatin sensitivity in OVCAR3 cell lines, while having the opposite effect on SKOV3 ovarian cancer cell lines. We speculate the observed effects are related to an interaction of heparin with signal transduction molecules.

Survivors of Endometrial Cancer: Who is at Risk for Sexual Dysfunction?

Nonyem Onujiogu, MD Tasha Johnson, MD, Songwon Seo, Katherine Mijal, BS, Joanne Rash, PA-C Lori Seaborne, PA-C Stephen Rose, MD David Kushner, MD

Objective: Given the prevalence of endometrial cancer, there is surprisingly limited data examining sexual function in this patient population. This may be because these patients are thought to be at low risk for this problem. Research on sexual dysfunction has increased in gynecologic oncology but has mostly focused on women with cervical cancer. Our aim is to determine the prevalence of sexual dysfunction and identify risk factors associated with sexual morbidity in patients treated for early stage endometrial cancer. Materials: This prospective trial included patients with stage I-IIIa endometrial cancer, without evidence of disease, one to five years out from primary surgical treatment. Patients who received chemotherapy were excluded. The Female Sexual Function Index (FSFI) was used to measure our primary endpoint of sexual function. Other patient reported outcome indices used to define this population included Functional Assessment of Cancer Therapy-Endometrial (FACT-En), Center for Epidemiology Studies Depression scale (CES-D), and Menopausal Rating Scale (MRS). Results: Of the 73 women treated for early stage endometrial cancer at our academic medical center, 60% were married, 49% had a sexual partner, the mean age was 60, 86% had stage I disease, and 18% received radiation therapy. The median score for the FSFI was 16.6 (0-32.8; scores below 26 are diagnostic for sexual dysfunction). Eighty nine percent of the patients had a score below 26. Among the subcategories of sexual dysfunction, pain was the most dramatically affected. Univariate analysis revealed a significant correlation between the total FSFI score and radiation therapy, histologic grade, current use of vaginal dilators, relationship status, mental health, heart disease and diabetes. There was a significant correlation between the total FSFI score and FACT-En scores but not with CES-D or MRS scores. After multivariate analysis, grade, sexual partner, heart disease, mental health, and diabetes remained significant. Conclusions: Our findings suggest that this patient population commonly thought to be at low risk actually suffers from severe sexual dysfunction when compared to the general population. The five risk factors revealed by multivariate analysis need to be studied in greater detail in order to appropriately target patients and develop meaningful interventions.

17β-estradiol-induced Temporal and Spatial Partitioning of eNOS and Estrogen Receptors in Ovine Uterine Artery Endothelial Cells from Pregnant Sheep

Mayra B. Pastore1, Jayanth Ramadoss1, Wu-xiang Liao2, Dong-bao Chen2, Ronald R. Magness1 1Perinatal Research Laboratories, Depts. of Ob/Gyn, University of Wisconsin-Madison, Madison, WI, 53715 and 2Department of Obstetrics & Gynecology, University of Cali

BACKGROUND: Pregnancy-induced elevations in uterine blood flow are closely correlated with concurrent increases in plasma 17β-estradiol levels and the expression/activity of eNOS. We have recently reported that eNOS is partitioned between caveolar and non-caveolar domains in pregnant uterine artery endothelial cells (UAECs) and this enzyme exhibits domain-specific post-translational modification via multi-site phosphorylation. We further have shown that the calcium mobilizing agonist ATP re-partitions eNOS between cellular domains and alters the phosphorylation state. HYPOTHESIS: We hypothesized that 17β-estradiol-induced eNOS activation via the non-classical ER receptor will initiate the sequential and coordinated re-partitioning and activation of eNOS with an altered multi-site phosphorylation state. METHODS: UAECs were isolated from primary uterine arteries of pregnant ewes (gestational day 120-130). Confluent passage 4 cells were treated in media without (Control) or with 17β-estradiol (10 nM) for 10 minutes. The caveolae were fractionated from cells using sucrose density gradient centrifugation. Immunoblotting was utilized to study the multi-site phosphorylation state of eNOS and ERs. RESULTS: In control UAECs, eNOS was significantly higher in the caveolar domain when compared to 17β-estradiol-treated cells. In control cells, stimulatory P635eNOS and P1177eNOS were not detected in any of the fractions whereas inhibitory P114eNOS was detected strictly in the non-caveolar domain. In response to 17β-estradiol, stimulatory P635eNOS was detected in all cellular domains whereas p1177eNOS was detected mainly in the caveolar domain and inhibitory P114eNOS was detected in low levels in the non-caveolar domain. Both ERα and ERβ were mainly detected in the non-caveolar domain in control cells whereas ERβ was also detected in the caveolar domain but at lower levels. 17β-estradiol did not alter the distribution of the ERs. CONCLUSIONS: 17β-estradiol produces temporal and spatial re-partitioning of eNOS from the caveolar to non-caveolar domains and alters this enzyme's multi-site phosphorylation state and their distributions in UAECs. Furthermore, the similarities of these results to the ATP-responses illustrate alternative activation pathways of calcium mobilizing agonists. These findings are critical to understand 17β-estradiol-induced gestational vascular adaptations. NIH R25 GM083252, HL49210, HL87144, HD38843, HL74947, HL70562 and HD58242

Effect of Chronic Binge Alcohol on NO Regulation and the Profile of NO-Related Caveolar Proteins in Ovine Pregnant Uterine Endothelial Cells

J Ramadoss, WX Liao, DB Chen, RR Magness

Pregnancy-induced coordinated growth and remodeling of the uterine circulation is intricately regulated by nitric oxide (NO) and the enzyme activity of eNOS. We investigated the effect of chronic binge alcohol on the signature profile of proteins embedded in endothelial caveolar microdomains, the natural home of eNOS. To mimic maternal binge drinking patterns, uterine artery endothelial cells were cultured in the absence or presence of alcohol (150 mg/dl) in sealed, humidified chambers equilibrated with aqueous alcohol for 3 h on 3 consecutive days. Isolated caveolae were analyzed by mass spectrometry. Cell viability was validated. Binge alcohol significantly decreased eNOS protein (-57%), activated eNOS (P635eNOS, -85%), and the eNOS-regulating ERK signaling cascade (total ERK1, -84%; ERK2, -79%; pERK1, -76%). Uterine vascular specificity was demonstrated as the commonly implicated AKT pathway was unaltered. Binge alcohol altered the array of caveolar proteins; a distinctive signature profile was observed with several abundant caveolar proteins being dramatically decreased or knocked out. Alcohol resulted in decreases in the abundance of caveolar proteins related to adhesion (-29%), cell function (-53.3%), signaling (-57.2%), deubiquitination (-51.5%), histones (-13.2%), nitric oxide (NO) regulation (-60.2%), structure (-36.4%), and transport/trafficking (-53.3%). The only protein that exhibited a significant increase in response to alcohol was fibronectin (+164%). Caveolar proteins related to NO regulation including HSP70 V, cav-1, and eNOS were decreased by 65%, 59%, and 51% respectively. The major deubiquitination enzyme USP2 was decreased by 52%. Immunoblot validation of protein changes compartmentalized to the caveolae including cav-1 and eNOS confirmed and validated proteomic findings. Whole cell eNOS level was comparable between proteomics (-59%) and immunoblotting (-57%). 1. These data demonstrate that the uterine vascular endothelial caveolar assemblage of proteins may influence eNOS abundance and activity. 2. The dramatic alteration in all proteins associated with NO regulation suggests major uterine vascular effects of alcohol. 2. ERK cascade specifically regulates uterine vascular eNOS. 3. Alterations in deubiquitination enzymes may form the mechanistic basis for alcohol-induced caveolar profile. 5. Finally, the profile suggests an important role for the utero-placental compartment in FASD. NIH HL49210, HD38843, HL87144, HL86939.

Mamu-AG Modulation of Decidual Macrophage Function

A. Rozner, R. Durning, S. Dambaeva, J. Drenzek, and T. Golos

At the time of implantation and throughout pregnancy, the primate uterus contains numerous leukocytes, consisting primarily of natural killer cells and macrophages. These cells are thought to play an important role in the maternal fetal immune response. The cytokine balance at the maternal fetal interface and the expression of non-classical MHC class I molecules (HLA-G in humans and Mamu-AG in the rhesus monkey) on the trophoblast cells of the growing embryo are thought to be important immune modulators that allow the semi-allogenic embryo to implant and optimize the environment for placental and fetal growth. Rhesus monkey decidual macrophages were co-cultured with Mamu-AG expressing trophoblasts isolated from the day 36 placenta. Macrophage functions including DC-SIGN expression, antigen uptake and processing ability, and cytokine secretion were evaluated. An increase in secretion of IL-6 and IL-18 and a decrease in secretion of MIP-1alpha and MIP-1beta were noted. When trophoblasts were treated with a Mamu-AG blocking antibody, 25D3, the decrease in MIP-1alpha and MIP-1beta was blocked. These results suggest Mamu-AG may be involved in regulating decidual macrophage production of MIP-1alpha and MIP-1beta.

Insulin Resistance Impairs Post-Receptor Signaling Mechanisms in Ovarian Cells

Soraya S. Arriaga, Milo Wiltbank

Polycystic ovary syndrome (PCOS) is a reproductive abnormality that affects 5-10% of women of child bearing age. PCOS is characterized by amenorrhea or oligomenorrhea, anovulation, and hyperandrogensim. One third of women with PCOS are insulin resistant (IR) and one out of ten diabetic women has PCOS. In previous studies of different cell types, it was shown that in PCOS women with IR and in IR individuals' alike, defects in post receptor signaling mechanisms impaired insulin action. We hypothesize, that in the ovary, the signaling impairment that occurs in IR states may also affect the IGF-1 system. Interrelated abnormalities of the IGF-1 signaling system and ovarian steriodogenesis may be vital in the arrested state of follicle development. Objective: 1) Induce insulin resistance in ovarian cells in vitro, 2) Study insulin and IGF-1 post-receptor signaling. Methods: Isolate and culture bovine granulosa and thecal cells. Insulin resistance will be attained using: 1) Physiological levels of insulin, previously determined in an in vivo model for insulin resistance, 2) Fatty acids 3) Blocking key insulin pathways using inhibitors for signaling factors. Insulin resistance will be assessed by glucose uptake and investigation of protein content, activity and phosphorylation of molecular mediators of insulin signaling.

Iron Binding Proteins in Human Milk in the First 10 Postpartum Days

V. Sridhar, E. L. Edde, L. L. Ngo, P. J. Kling

Background: Lactoferrin (Ltf), transferrin (Tf) and ferritin (Ferr) are major iron-binding proteins, though their precise role in iron transport in human colostrum or milk is unknown. While it is widely established that Ltf levels decreases in breast milk with increasing postpartum age, the trend of Tf and Ferr has not been investigated in detail during early lactation. Purpose of study: We hypothesized that the magnitude abundance of major iron-binding proteins Ltf, Tf and Ferr in breast milk will decrease with increasing postnatal days and that their levels will directly correlate with milk iron levels. Methods: Measurable immunoreactive Ltf, Tf and Ferr concentrations were determined utilizing ELISA and immunoradiometric assays in 196 human milk samples obtained in the first 10 postpartum days (PD) from mothers of 35 term and 37 premature infants. Further, total iron was measured using spectrophotometric assays. Results: Milk-borne Ferr abundance levels were significantly greater on PD 0 and 1 compared with that measured between PD 2 through 10 ($p<0.0001$). Ltf and Tf also exhibited a similar trend ($p<0.0001$); levels declined on PD 3. Consistent with literature, iron content of the milk samples also decreased as postnatal day increased ($p<0.0005$). Significant correlations were noted between breast milk iron and Ltf ($p<0.0001$) and Ferr ($p<0.0028$) levels. However, in a multiple stepwise regression, only ferritin was correlated to milk iron. No differences were observed in any of the dependent measures between premature and term groups. Conclusion: These results demonstrate that the three iron-binding proteins Ltf, Tf and Ferr may play a significant role in iron transport during early lactation. Further, Ltf and Tf exhibits a sharp decline in their magnitude on PD 3 and Ferr levels dramatically decline on PD2, suggesting that the critical window during early lactation for iron transport proteins could be explained by paracellular transport between mammary epithelial cells. This would require further study.

Studying the importance of MUC16-Siglec-9 binding on the function of NK cells in preeclampsia

Chanel Tyler, Arvinder Kapur, Jenifer A. Belisle, Joseph P. Connor, Manish S. Patankar

Pregnancy is a state in which the fetal allograft is safeguarded from rejection by the maternal immune system. NK cells are the major immunologic cell in the first trimester during trophoblastic invasion. NK cell cytokine secretion has previously been shown to be integral to the successful implantation, as well as trophoblastic invasion. Pregnancy cytokine profiles have demonstrated repeatedly that there is a Th1 (pro-inflammatory) bias although success of pregnancy does not mandate this shift. This bias towards the pro-inflammatory Th1 response is exaggerated in preeclampsia. For several years the Th1/Th2 paradigm dominated the field. However the simplicity of this model has led it to be called into question. MUC16 has previously been shown to immunomodulate NK cell function in ovarian cancer. This mucin has also been shown to bind to NK cells during pregnancy. Our study was designed to investigate the hypothesis that there is a spectrum of MUC16 binding that correlates to the level of inflammation. We proposed that MUC 16 binding increases throughout the course of pregnancy acting as a modulator of the inflammatory response. Our study was conducted on peripheral blood and decidual immune cells isolated at term from women with healthy pregnancy and preeclampsia. All subjects signed an informed consent, and the study was approved by the Institutional Review Boards at the University of Wisconsin-Madison and Meriter Hospital. The women were recruited at the time of admission to Labor and Delivery. Maternal serum obtained at 0-12 weeks, 28 weeks, and at delivery from cytometry. Mononuclear cells were isolated using Histopaque. The MUC16 and Siglec9 expression of the cells was characterized by multi-color flow cytometry using an LSR-II. We observed a difference in the binding of MUC16 to NK cells isolated from healthy pregnant women as compared to preeclamptics. A corresponding difference was also observed in the expression of the MUC16 receptor, Siglec-9, on the NK cells of women with preeclampsia. As the fetal allograft grows, there is an increased need for immunomodulation of NK cells and, therefore, aberrant binding of MUC16 and expression of Siglec-9 may have important physiologic consequence. We believe that this finding will not only hold true but be exaggerated when evaluating preeclamptics secondary to the exaggerated inflammation seen in this condition. To understand the biology of MUC16-Siglec-9 binding and its effects on NK cell function, we are using the NK cell leukemia cell line NKL as a model and have utilized several approaches to transfect these cells with human Siglec-9. Studies on the effect of Siglec-9 on NK cell function will be described.

"Yin-Yang" Principle for Estrogen Receptor Heterodimers in Breast Cancer: A Targeted Molecular Approach for Therapeutic Development.

Emily Powell, Noel Peters, Michael Hoffmann, and Wei Xu

Estrogen receptor (ER) dimerization is prerequisite for its activation of target gene transcription. Since the two forms of ER, ERalpha and ERbeta, exhibit opposing functions in cell proliferation, the ability of ligands to induce ERalpha/beta heterodimers versus their respective homodimers is expected to have profound impacts on transcriptional outcomes and cellular growth. However, there is a lack of direct methods to monitor the formation of ERalpha/beta heterodimers in vivo and to distinguish the ability of estrogenic ligands to promote ER homo- versus hetero-dimerization. Here we describe the identification of estrogenic small molecule ER ligands by high throughput transcriptional activation assays and the subsequent characterization of these compounds using secondary Bioluminescence Resonance Energy Transfer (BRET) screening assays. While the primary transcriptional activation assays allowed determination of transcriptional activation specific to ERs, it did not allow determination of ER subtype specificity. Thus, we employed the BRET assay for monitoring the formation of ERalpha/beta heterodimers and their respective homodimers in live cells. Using this two-step screening of small molecule libraries, we identified several bioactive compounds capable of inducing ERβ/β homodimers and ERα/β heterodimers while having minimal activity on pro-proliferative ERα/α homodimers, posing a model that compounds promoting ERalpha/beta heterodimer formation might have therapeutic value. The biological effects of ERalpha/beta-selective compounds in a variety of normal and tumorigenic cell lines derived from hormone-dependent cancers support this notion. Thus, our three step screening process of transcriptional transactivation assays, BRET assays, and cell-based biological function assays is applicable to drug screening for dimer-selective SERMs, which uniquely target ERalpha/beta heterodimers in cancer cells. Supported by NIH T32 CA009135; R01 CA125387; The University of Wisconsin Graduate School; Wisconsin Alumni Research Foundation Lead Discovery Initiative.

2010 ERP Program Faculty Directory

Name	Department	Address	Phone #	E-Mail
Abbott, David **Professor**	Primate Center; Obstetrics & Gynecology	203 Primate Center 1220 Capitol Court	263-3583	abbott@primate.wisc.edu
Alarid, Elaine **Associate Professor**	Oncology	710 McArdle Cancer 1400 University Ave.	265-9319	alarid@oncology.wisc.edu
Atwood, Craig **Associate Professor**	Medicine	D4219 VA Hospital 2500 Overlook Terrace	256-1901	csa@medicine.wisc.edu
Barry, Terence **Senior Scientist**	Animal Sciences; Aquaculture Program	656 Animal Sciences 1675 Observatory Dr.	263-2087	tpbarry@wisc.edu
Bertics, Paul **Professor**	Biomolecular Chemistry	571A Medical Sciences Center 1215 Linden Drive	262-8667	pbertics@wisc.edu
Bird, Ian (Program Director) **Professor**	Obstetrics & Gynecology	7E Meriter Hospital 202 South Park Street	417-6314 417 -6252	imbird@wisc.edu
Blank, Robert **Associate Professor**	Medicine	Box 5148 Clinical Science Center-H4, 600 Highland Ave	263-9221	rdb@medicine.wisc.edu
Bosu, William **Professor**	Medical Sciences	2031 Veterinary Medicine 2015 Linden Drive	263-7752	bosuw@svm.vetmed.wisc.edu
Downs, Karen **Professor**	Anatomy	263 Bardeen Medical Labs 1300 University Avenue	265-5411	kdowns@wisc.edu
Drezner, Marc **Professor**	Medicine	Box 5148 CSC-H4 600 Highland Ave	263-9221	mkd@medicine.wisc.edu
Duello, Theresa **Associate Professor**	Obstetrics & Gynecology	5240 Medical Sciences Center 1300 University Avenue	262-7456	tmduello@wisc.edu
Cezar, Gabriela **Assistant Professor**	Animal Sciences	752 Animal Sciences 1675 Observatory Dr.	263-4307	ggcezar@wisc.edu
Ginther, Oliver **Professor**	Pathobiological Sciences	B1 Animal Health & Biomedical Sc. 1656 Linden Drive	262-1037	ojg@ahabs.wisc.edu
Golos, Thaddeus **Professor**	Comparative Biosciences	115 Primate Center 1220 Capitol Court	263-3567	golos@primate.wisc.edu
Jefcoate, Colin **Professor**	Pharmacology	5007 Wisconsin Institutes Medical Research 1111 Highland Ave.	263-3975	jefcoate@wisc.edu
Jorgensen, Joan **Assistant Professor**	Comparative Biosciences	4354c Veterinary Medicine Building, 2015 Linden Dr	890-2337	jsjorgensen@wisc.edu
Kessel, Julie **Associate Professor (CHS)**	Pediatrics	6 Center Meriter Hospital 202 S. Park St.	417-6236	jmkessel@wisc.edu

Name	Department	Address	Phone #	E-Mail
Kling, Pamela **Associate Professor**	Pediatrics	6 C Meriter Hospital 202 South Park St.	262-6561	plking@wisc.edu
Khatib, Hasan **Associate Professor**	Dairy Sciences	632 Animal Science Building, 1675 Observatory Dr	263-3484	hkhatib@wisc.edu
Kreeger, Pamela **Assistant Professor**	Biomedical Engineering	2154 Engineering Centers 1550 Engineering Dr	890-2915	kreeger@wisc.edu
Magness, Ronald **Professor**	Obstetrics & Gynecology	7E Meriter Hospital 202 South Park Street	417-6314 417-6498	rmagness@wisc.edu
Martin, Thomas **Professor**	Biochemistry	5519 Biochemistry 420 Henry Mall	263-2427	tfmartin@wisc.edu
Ntambi, James **Professor**	Biochemistry & Nutritional Sciences	180A Biochemistry 420 Henry Mall	265-3700	ntambi@biochem.wisc.edu
Odorico, Jon **Associate Professor**	Surgery	H4/756 Clinical Science Center, 600 Highland Ave	265-6471	jon@surgery.wisc.edu
Parrish, John **Professor**	Animal Science	714 Animal Sciences Building, 1675 Observatory Drive	263-4324	parrish@ansci.wisc.edu
Patankar, Manish **Associate Professor**	Obstetrics & Gynecology	Box 6188 CSC-H4 600 Highland Ave	262-8871	patankar@wisc.edu
Peterson, Richard **Professor**	Pharmacy	5109 Rennebohm Hall 777 Highland Ave.	263-5453	repeter- son@pharmacy.wisc.edu
Salih, Sana **Assistant Professor**	Obstetrics & Gynecology	Box 6188 Clinical Science Center-H4 600 Highland Ave	263-1218	salih@wisc.edu
Schuler, Linda **Professor**	Comparative Biosciences	4354/B Veterinary Medicine Bldg. 2015 Linden Drive	263-9825	schul- erl@svm.vetmed.wisc.edu
Shah, Dinesh **Professor**	Obstetrics & Gynecology	6 Center, Meriter Hospital 202 South Park Street	417-6618	dmshah@wisc.edu
Shalev, Anath **Associate Professor**	Medicine	Box 5148 Clinical Science Center -H4, 600 Highland Ave	263-9221	as7@medicine.wisc.edu
Terasawa, Ei **Professor**	Pediatrics; Primate Center	217 Primate Center 1223 Capitol Court	263-3579	terasawa@primate.wisc.edu
Thomson, James **Professor**	Anatomy; Primate Center	425 Henry Mall	263-3585	thomson@primate.wisc.edu

Name	Department	Address	Phone #	E-Mail
Vezina, Chad **Assistant Professor**	Comparative Biosciences	121 Animal Health & Biomedical Sciences Bldg 1656 Linden Dr	890-3235	cmvezina@wisc.edu
Watters, Jyoti **Associate Professor**	Comparative Biosciences	4470 Veterinary Medicine 2015 Linden Drive	262-1016	jjwatters@wisc.edu
Wiltbank, Milo **Professor**	Dairy Science	856 Animal Sciences 1675 Observatory Drive	263-9413	wiltbank@wisc.edu
Zheng, Jing **Associate Professor**	Obstetrics & Gynecology	7 E. Meriter Hospital 202 S. Park St.	417-6226	jzheng@wisc.edu

2010 ERP Program Student Directory		
NAME	**ADVISOR**	**EMAIL**
Alvarez, Roxanne	Bird, Ian M.	realvarez@wisc.edu
Bankowski, Heather	Bird, Ian M.	hkerrick@wisc.edu
Boeldt, Derek	Bird, Ian M.	dsboeldt@wisc.edu
Bushkofsky, Justin	Jefcoate, Colin R.	bushkofsky@wisc.edu
Clemente, Luca	Bertics, Paul John	lclemente@wisc.edu
Giakoumopoulos Maria	Golos, Thaddeus G.	giakoumopoul@wisc.edu
Guerriero,Kathryn	Terasawa-Grilley, Ei	kguerriero@wisc.edu
Hackbart, Katherine	Wiltbank, Milo C.	khackbart@wisc.edu
Hayashi, Kentaro	Atwood, Craig S	hayashi3@wisc.edu
Hutcherson, Beverly	Abbott, David H.	bahutcherson@wisc.edu
Jiang, Yizhou	Zheng, Jing	jiang5@wisc.edu
Jobe, S. Omar	Magness, Ronald R.	sjobe@wisc.edu
Kenealy, Brian	Terasawa-Grilley, Ei	kenealy@wisc.edu
Kibbe, Carly	Shalev, Anath	kibbe@wisc.edu
Kristianto, Jasmin	Duello, Theresa	kristianto@wisc.edu
Krupp, Jennifer	Bird, Ian M.	jlkrupp@wisc.edu
Lee, Jinwoo	Jefcoate, Colin R.	jwlee7@wisc.edu
Lewis, Samantha	Jorgensen, Joan	srlewis2@wisc.edu
Li, Yan	Duello, Theresa	li99@wisc.edu
Maguire, Meghan	Bird, Ian M.	mlmaguire@wisc.edu
Meyer, Katie	Bird, Ian M.	kmmeyer1@wisc.edu
Morschauser, Timothy	Bird, Ian M.	morschauser@wisc.edu
Nair, Gopika	Odorico, Jon S.	gnair@wisc.edu
Pastore, Mayra	Duello, Theresa	mpastore@wisc.edu
Rozner, Ann	Golos, Thaddeus G.	annbaker@wisc.edu
Silva, Soraya	Wiltbank, Milo C.	ssilva@wisc.edu
Tyler, Chanel	Patankar, Manish S	cttyler@wisc.edu

NIH T32 Trainees 2004-Present	
Dr. Jennifer Arens-Gubbels, PhD	Derek Boeldt
Dr. Jacqueline Cale, PhD	Justin Bushkofsky
Dr. Jessica Drenzek, PhD	Maria Giakoumopoulos
Dr. Behzad Gerami-Naini, PhD	Kathryn Guerriero
Dr. Nichole Korpi Steiner, PhD	Katherine Hackbart
Dr. Sekoni Noel, PhD	Samantha Lewis
Dr. J. Christina Pattison, PhD	Ann Rozner
Dr. Amy Reeder, PhD	Dr. Chanel Tyler